Journal of the Optical Society of Korea
Vol. 15, No. 1, March 2011, pp. 38-43

DOI: 10.3807/JOSK.2011.15.1.038

Simple Model of Bright-room Contrast Ratio Measurement System for Plasma Display Panels with Contrast Enhancement Film

Tae Won Beom

DS LCD Co., LTD., 583-2 Gumgok-ri, Dongtan-myun, Hwaseong 445-811, Korea

Gi Chan Park and Jong Rak Park*

Department of Photonic Engineering, Chosun University, Gwangju 501-759, Korea

Youngsik Kim and Jun Zhang

College of Optical Sciences, University of Arizona, Tucson, Arizona 85721, USA

Bu Seup Song, Jong Pil Chun, and Ki Cheol Yoon

Samsung Fine Chemicals Company, Daejeon 305-380, Korea

Won-Gun Jang

Korea Photonics Technology Institute, Wolchul-dong, Buk-gu, Gwangju 500-460, Korea

(Received January 24, 2011 : revised February 22, 2011 : accepted February 23, 2011)

We have developed a simple model of a bright-room contrast ratio (BRCR) measurement system for plasma display panels (PDPs) adopting a contrast enhancement film (CEF) by using an illumination design tool. Only four model parameters were used, namely, total ambient illumination power delivered by fluorescent lamps, a panel scattering rate, illuminance of PDP white patterns, and the absorption coefficient of a color adjusting film. These parameters were determined by simple optical measurements and matching simulations. The proposed model was employed to predict the BRCR values of four different CEF samples, and the simulated ones were found to be in agreement with measured ones within about 10% relative-error.

Keywords : Plasma display panel, Contrast enhancement film, Bright-room contrast ratio, Illumination design

OCIS codes : (120.2040) Displays; (120.3930) Metrological instrumentation; (220.2945) Illumination design

I. INTRODUCTION

Among the various flat display devices, plasma panel displays (PDPs) have attracted considerable attention because they are self-emitting devices that exhibit inherently good optical characteristics, including high dark-room contrast, high brightness, and a wide viewing angle [1, 2]. PDPs employ front filters or PDP filters in order to achieve many important optical and other properties, such as shielding unwanted electronic interference, eliminating ultraviolet (UV) radiation, cutting infrared emission, and correcting color [3-5]. Because of the ever-increasing demand for a high bright-room contrast ratio (BRCR), contrast enhancement films (CEFs) are commonly adopted into PDP filters [4-7].

Several studies have been conducted on the modeling and simulation of either the discharge characteristics for PDPs [8-11] or optical characteristics for liquid crystal displays adopting various optical films [12-15]. However, to the best of our knowledge, the modeling and simulation of the optical characteristics of PDPs, including the BRCR

*Corresponding author: ejrpark@chosun.ac.kr

Color versions of one or more of the figures in this paper are available online.

performance, has not yet been reported. In this study, we have carried out a simplified modeling of a BRCR measurement system and simulated BRCR values for a PDP module adopting CEF samples by using an illumination design tool. We mention that the model and simulation procedures reported in this paper are not restricted to the design tool.

In the next section, we describe the BRCR measurement system and the model in detail. In Section 3, we present the structural and optical parameters of CEF samples considered in this study and compare the results of a simulation of BRCR values of the samples with those of measurements of these values. Finally, in Section 4, we present the conclusions with a brief summary.

II. MODEL FOR BRCR MEASUREMENT SYSTEM

2.1. BRCR and Its Measurement System

Figure 1 shows a layout of a typical BRCR measurement system that consists of a luminance meter (spectroradiometer), fluorescent lamps (source of ambient light), and a PDP module. The BRCR of a PDP module is defined as the ratio of the luminance of a white pattern to that of a black window under bright-room conditions [16]. In general, the luminance measured for the black window is much smaller than that of the white pattern; therefore, the BRCR highly depends on the luminance of the black window that results from the ambient light.

We used diffuser sheets around the fluorescent lamps to adjust the illuminance by ambient light at the center of the PDP module to 150 lx, which is a typical bright-room constraint in the industry [17]. Once the bright-room condition is set up, the subsequent procedure is to measure the luminance of the PDP module (L_{OFF}) under ambient illumination when the white pattern is turned off. The luminance of the PDP module (L_{ON}) is then measured with the white pattern turned on and with ambient illumination. Finally, we calculate the BRCR value from the ratio of the measured luminance values (L_{ON} /L_{OFF}). For the experiments reported herein, the white pattern was a 114 mm × 64 mm rectangular radiation window, which was placed at the center of the module.

For this study, we used a 50-inch PDP module, 3 fluorescent lamps, and a spectroradiometer (CS-2000, Konica Minolta). The BRCR measurement standard requires the measurement distance between the PDP module and the luminance meter to be 1.6 V~2.8 V from the luminance meter, where V represents the vertical length of the PDP module [16]. For our experiment and simulation, the distances H_I, H_{II}, L_I, and L_{II} (see Fig. 1) were 710 mm, 1180 mm, 750 mm and 740 mm, respectively. The distance between the PDP module and the luminance meter was 1490 mm, which corresponds to 2.4 V and thus satisfies the standard.

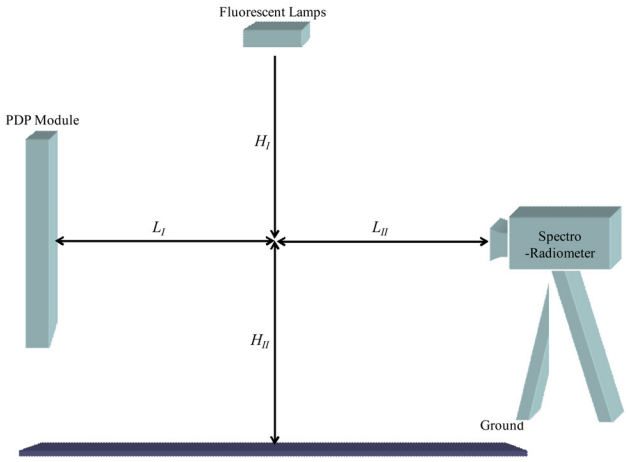

FIG. 1. Layout of a typical BRCR measurement system.

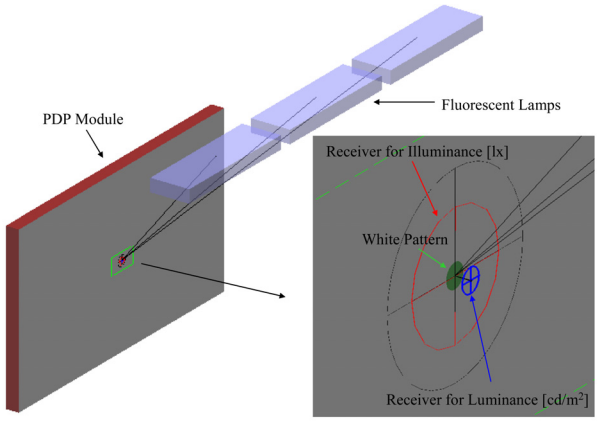

FIG. 2. Layout of the BRCR measurement system modeled with *LightTools*.

2.2. Model Description

Figure 2 shows a layout of a BRCR measurement system model. A fully-physical model of the measurement system, which takes into account all the details of structural and optical properties of constituent elements of the measurement system, would be desirable. However, the modeling itself and the simulations using the fully-physical model are not practical and almost unfeasible due to the structural and optical complexity of the system. We modeled the BRCR measurement system in as simple a manner as possible as a first step toward a practical model which can be utilized for designing CEFs of high performance.

In our model, developed and simulated by using an illumination design tool *LightTools* (Optical Research Associates), all light sources including fluorescent lamps and the white pattern of the PDP module are assumed to be Lambertian and monochromatic (555 nm); the reflection and scattering properties of the PDP module are modeled solely by the Lambertian scattering property of the outer surface of the PDP module; and the optical property of the color adjusting film (CAF), on the top of which is attached the CEF, is

represented by volume absorption. Therefore, our model uses only the following four model parameters: flux of fluorescent lamps, scattering rate (total reflectance for Lambertian scattering) of the PDP module, illuminance of the white pattern, and absorption coefficient of the CAF. To determine the model parameter values, we performed simple optical measurements along with the matching simulations, which we will describe in detail shortly. In general, most scattering surfaces are closer to Gaussian scattering than to Lambertian scattering. In this study, the outer surface of the PDP module was assumed to have the Lambertian scattering property because of its simplicity. In order to employ the Gaussian scattering property, we need to determine the angular width in addition to the total reflectance of the Gaussian scattering, which will give additional complexity to our model. So, we tried the Lambertian scattering first. We mention that the model can be easily extended to take into account the spectral and angular distributions of the sources, the spectral and angular scattering property of the PDP module and the spectral absorption characteristic of the CAF.

In the model, we employ the real size of the PDP module (50 inch, 1120 mm × 630 mm) and the fluorescent lamps are modeled as three cube sources, each of which has dimensions of 500 mm × 150 mm × 50 mm. The model contains an illuminance receiver and a luminance receiver. The illuminance receiver has a radius of 12.85 mm, which reflects the real size of its experimental counterpart (T-10, Konica Minolta), and the luminance receiver has a diameter of 5 mm and a measuring angle of 1º, which also reflects the major specifications of the spectroradiometer (CS-2000, Konica Minolta) used in the experiments.

2.3. Determination of Model Parameters

In this section, we describe the procedure used to determine the values of the four modeling parameters introduced just above. First, we selected four measurable parameters (target parameters) that would be significantly affected by the model parameters: illuminance at the center of the PDP module by the ambient light only, luminance from the center of the bare PDP module (without a CAF) due to illuminance by the ambient light only, luminance from the center of the bare PDP module due to illuminance by both the white pattern and the ambient light, and luminance from the center of the PDP module equipped with a CAF due to illuminance by the ambient light only. The four selected target parameters and the experimental conditions under which they were measured are summarized in Table 1, with the experimentally determined values of the target parameters being listed in the fifth column of Table 1.

The values of the four model parameters were determined by matching simulations, the results of which are shown in Fig. 3. First, we simulated the illuminance at the center of the PDP module (the first target parameter) as a function of the total flux of the fluorescent lamps [the first model parameter, see Fig. 3(a)]. We find that the result of the simulation matches the experimental result for the illuminance at the center of the PDP module (i.e., 150 lx) when the total flux of the fluorescent lamps is 1910 lm, which is the value of the first model parameter as determined by the matching simulations. Next, we fixed the first model parameter to be 1910 lm and simulated the luminance from the center of the PDP module (second target parameter) as a function of the scattering rate of the PDP module [second model parameter, see Fig. 3(b)]. From the simulation results, the value of the second model parameter was determined to be 21.63%. In the same manner, the third (illuminance of the white pattern) and the fourth (absorption coefficient of the CAF) model parameters were determined to be 3930 lx and 0.0173 μm^{-1}, respectively [see Figs. 3(c) and (d)]. In the model, the CAF thickness was 10 μm, which was a typical value for the CAF used for the experiment.

TABLE 1. Summary of target and model parameters

Experimental Condition			Target Parameter		Model Parameter	
CAF	Fluorescent Lamp	White Pattern	Parameters	Measured Values	Parameters	Model Values
Without	ON	OFF	Illuminance at the Center of PDP Module	150 lx	Flux of Fluorescent Lamp	1910 lm
	ON	OFF	Luminance from the Center of PDP Module	10.35 cd/m^2	Scattering Rate of Module	21.63 %
	ON	ON	Luminance from the Center of PDP Module	1255 cd/m^2	Illuminance of White Pattern	3930 lx
With	ON	OFF	Luminance from the Center of PDP Module	5.59 cd/m^2	Absorption Coefficient of CAF	0.0173 μm^{-1}

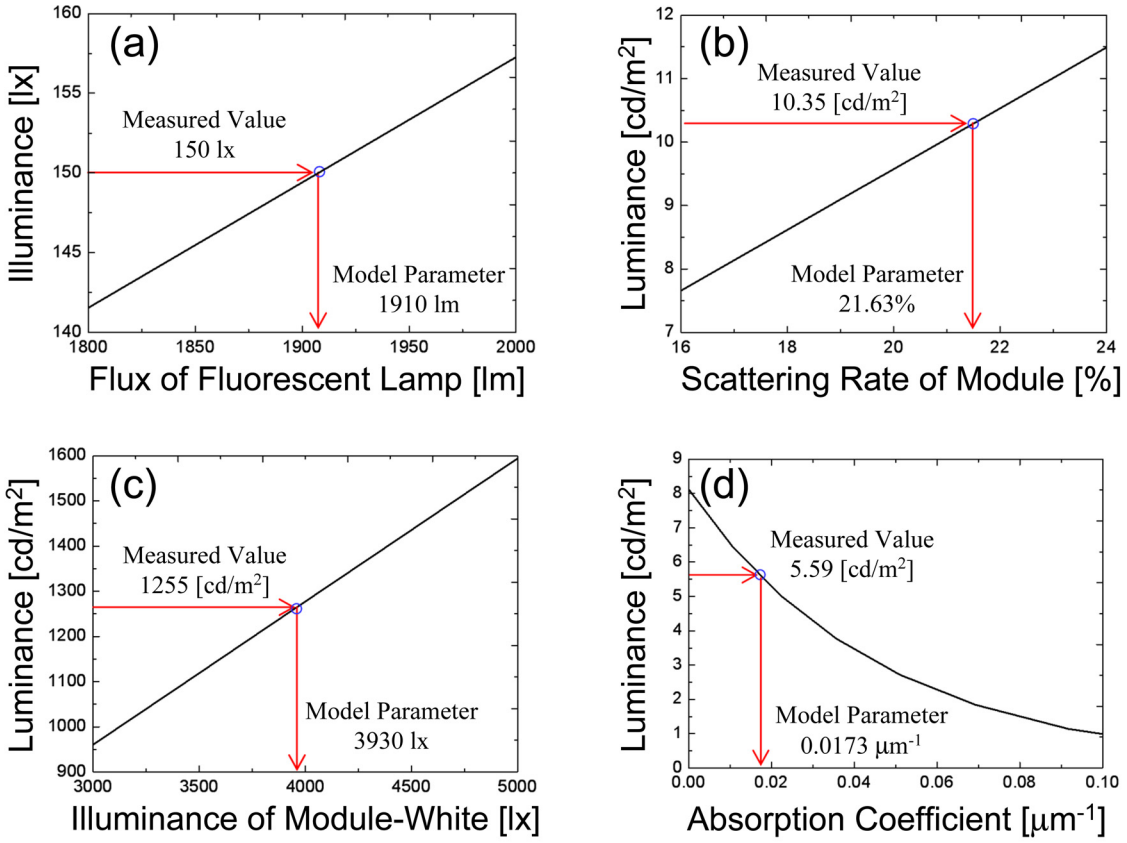

FIG. 3. Results of the matching simulations.

III. RESULTS AND DISCUSSION

3.1. Preparation of Contrast Enhancement Film Samples

In this section, we describe the CEF samples used for BRCR measurements. The CEF samples were composed of a substrate film (polyethylene terephthalate film) and an ultraviolet-curable (UV-curable) urethane acrylate layer that enclosed black stripes (BSs). The BSs, which are a group of trapezoidal structures made of a mixture of UV-curable urethane acrylate and carbon black (1.5 wt%), play a major role in CEFs by absorbing ambient light.

The samples were fabricated through a patterning process, a wiping process, and a curing process. In the patterning process, trapezoidal patterns were formed in the UV-curable urethane acrylate layer by using a metal mold with the desired microstructure patterns. In the wiping process, the trapezoidal grooves were filled with the BS solution (a mixture of UV-curable urethane acrylate and carbon black), and the surplus solution was wiped off with a blade. Finally, in the curing process, the prepared CEF samples were hardened by exposure to UV.

Figure 4 shows a cross-sectional schematic of the CEF samples, where t, b, d, p, k, and r represent the top-width, bottom-width, BS depth, pitch, thickness of a circular arc in the BS, and radius of this circular arc, respectively. After the wiping process, the circular arc structure at the top of the BSs was still visible. This was attributed to the fact that the UV-curable urethane acrylate layer was pressed by the blade to remove surplus BS solution during the wiping process. The layer recovered after the process. We

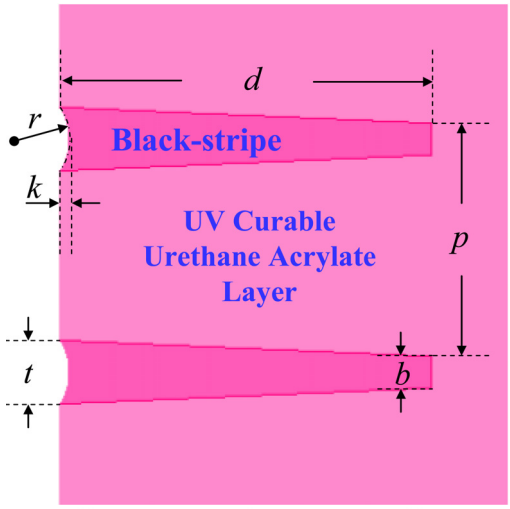

FIG. 4. Structure of a contrast-enhancement film, where t, b, d, p, k, and r represent top-width, bottom-width, BS depth, pitch, thickness of a circular arc in the BS, and radius of the circular arc, respectively.

TABLE 2. Summary of structural parameters for the fabricated CEF samples

Sample	t (mm)	b (mm)	d (mm)	p (mm)	k (mm)	r (mm)
A	0.010	0.006	0.053	0.031	0.001	0.009
B	0.022	0.006	0.102	0.073	0.003	0.020
C	0.022	0.006	0.105	0.073	0.003	0.020
D	0.020	0.010	0.123	0.074	0.003	0.018

TABLE 3. Simulation and experimental results for BRCR values for CEF samples

Sample	Experiment			Simulation		
	L_{ON} [cd/m^2]	L_{OFF} [cd/m^2]	BRCR	L_{ON} [cd/m^2]	L_{OFF} [cd/m^2]	BRCR
A	624.60	1.55	403	648.88	1.48	438
B	654.80	1.46	448	663.08	1.37	484
C	658.80	1.43	461	663.01	1.31	506
D	682.50	0.91	750	687.99	0.93	740

fabricated four types of CEF samples, whose structural parameters are given in Table 2. These parameters were measured by using microscope images of the samples' cross section. The absorption coefficient of the BSs was measured to be 0.0679 μm^{-1}, and the refractive indices of the urethane acrylate layer, the BSs, the substrate film, and the CAF were also measured to be 1.55, 1.56, 1.59, and 1.56, respectively. Those values were used for the simulations reported below.

3.2. Comparison of Simulation and Experimental Results

In this section, we present experimental and simulation results for the BRCR. We used the four types of CEF samples described in the preceding section to measure the BRCR values for the PDP module. Each CEF sample was attached to a CAF and placed in front of the PDP module. The gap between the PDP module and the CEF sample was 3 mm, and the wider side of the trapezoidal BS faced the PDP module.

The results of the measurements are listed in Table 3 along with results from the simulations, which were performed with the model described in Section 2 and which took into consideration the structural and optical parameters of each CEF sample. For the four CEF samples, the experimental results are within 10% of the simulation results for the BRCR values. Figure 5 shows these results in a graphical format, where the dotted lines represent the ±10% relative-error limit.

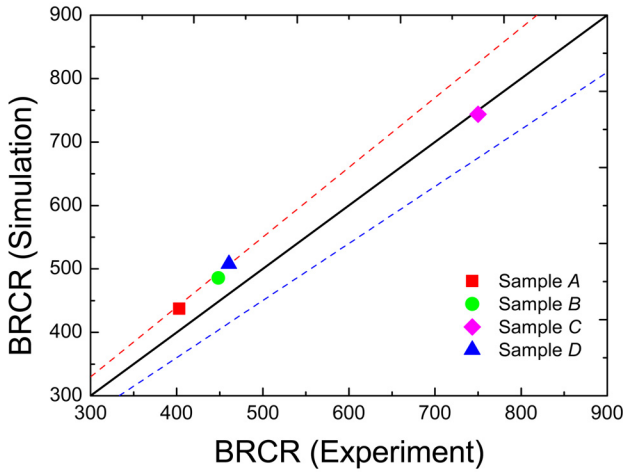

FIG. 5. Simulation and experimental results of the BRCR values for the four CEF samples. Dotted lines represent the ±10% relative-error limit.

The luminance of the PDP module with the white pattern turned on (L_{ON}) is mainly determined by the light coming from the white pattern, whereas the luminance with the white pattern turned off (L_{OFF}) is solely determined by the light from the fluorescent lamps. Because the angle of measurement of the luminance meter is 1°, nearly collimated light from the white pattern contributes to L_{ON}; hence, L_{ON} is closely related to the open ratio of the CEF structure [i.e., $(p - t)/p$]. The open-ratio values of the samples have the relationship of *A* (67.7%) < *B* (70.0%) = *C* (70.0%) < *D* (73.0%), and one can find that L_{ON} for the samples shows almost the same tendency.

In view of the experimental and simulation results, the

determination of L_{OFF} appears to be somewhat intricate. All the light from the fluorescent lamps has a large incident angle onto the CEF because of the geometry of the measurement system. While transmitting through the CEF, much of the light is absorbed in the BS structures. The transmitted light scatters off the PDP module and only the small portion directed almost normal to the CEF is detected by the luminance meter after passing through the CEF once again. Because L_{OFF} is strongly affected in a complicated manner by the structural parameters of the CEF, it appears very difficult to pick out from among them the most influential parameter. We believe, however, that it is possible to design a CEF with desirable properties by altering its structural and optical parameters.

IV. CONCLUSION

In this study, we have developed a simplified model of a BRCR measurement system for PDPs. This model uses only the following four parameters to design the BRCR measurement system: flux of ambient light sources, scattering rate of the PDP module, illuminance of the white pattern of the PDP module, and the absorption coefficient of the CAF. These parameters are uniquely determined by simple experiments and matching simulations.

We have fabricated four types of CEF samples and measured BRCR values of the PDP module adopting the CEF samples. The measured results were compared with the simulated results obtained by using the model. Although the model considered the spectral characteristics and the angular properties of the constituent parts of the BRCR measurement system in very simple ways, i.e., lumped at one wavelength and Lambertian, respectively, we found that these results were in good agreement for the four CEF samples considered in this study. The model will be used for the development of high-performance CEFs by optimizing its structural and optical parameters.

ACKNOWLEDGMENT

This study was supported by research funds from Chosun University, 2008.

REFERENCES

1. A. J. S. M. de Vaan, "Competing display technologies for the best image performance," J. Soc. Info. Display **15**, 9, 657-666 (2007).
2. Y. Sato, K. Amemiya, and M. Uchidoi, "Recent progress in device performance and picture quality of color plasma displays," J. Soc. Info. Display **10**, 17-23 (2002).
3. G. Zagdoun, T. Heitz, and X. Talpaert, "New type of optical filter for PDP TV with improved durability," SID Symposium Digest **35**, 918-921 (2004).
4. S.-H. Park, Y.-K. Lee, J.-D. Kim, J.-H. Kim, and H.-S. Cho, "Film for improving contrast and plasma display panel and display device including the same," U.S. Patent Pending 12/224550 (2007).
5. J. P. Chun, W. J. Jeong, K. C. Yoon, and B. S. Song, "Visibility enhancement film, display filter and display apparatus using the same," Korean Patent 0870290 (2008).
6. S. N. Cho, S. C. Jeong, and E. Y. Cho, "Light blocking layer, filter for display apparatus and display apparatus having the same," Korean Patent Pending 0132228 (2006).
7. E.-A. Moon, B.-W. Jeong, B.-J. Bae, J.-S. Kim, B.-G. Ryu, J.-S. Choi, and E.-C. Park, "Improvements made to the contrast ratio of PDPs in a bright room by coating the phosphors with pigments," SID Symposium Digest **39**, 186-189 (2008).
8. Y. Murakami, H. Matsuzaki, H. Murakami, and N. Ikuta, "Effective secondary electron yield of a cathode for plasma display panel," Jpn. J. Appl. Phys. **40**, 3382-3388 (2001).
9. T. Tamida, S. J. Sanders, and M. Tanaka, "Measurement and modeling of Xe vacuum ultraviolet emission and radiative transfer in a plasma display panel discharge," Jpn. J. Appl. Phys. **39**, 583-589 (2000).
10. T. Naoi, H. Lin, A. Hirota, E. Otani, and K. Amemiya, "Improved discharge characteristics using MgO single-crystal particles and advanced CEL structure," J. Soc. Info. Display **17**, 113-119 (2009).
11. T. Akiyama and T. Yamada, "Discharge analysis of high-efficacy PDP with a luminous efficacy of 5 lm/W," J. Soc. Info. Display **17**, 121-130 (2009).
12. G.-J. Park, Y.-G. Kim, J.-H. Yi, J.-H. Kwon, J.-H. Park, S.-H. Kim, B.-K. Kim, J.-K. Shin, and H.-S. Soh, "Enhancement of the optical performance by optimization of optical sheets in direct-illumination LCD backlight," J. Opt. Soc. Korea **13**, 152-157 (2009).
13. S.-H. Baik, S.-K. Hwang, Y.-G. Kim, G.-J. Park, J.-H. Kwon, W.-T. Moon, S.-H. Kim, B.-K. Kim, and S.-H. Kang, "Simulation and fabrication of the cone sheet for LCD backlight application," J. Opt. Soc. Korea **13**, 478-483 (2009).
14. M.-Y. Yu, B.-W. Lee, J. H. Lee, and J.-H. Ko, "Correlation between the optical performance of the reflective polarizer and the structure of LCD backlight," J. Opt. Soc. Korea **13**, 256-260 (2009).
15. J. H. Lee, T. Kim, T.-H. Yoon, J. C. Kim, C. G. Jhun, and S.-B. Kwon, "Transflective dual operating mode liquid crystal display with wideband configuration," J. Opt. Soc. Korea **14**, 260-265 (2010).
16. International Electrotechnical Commission (IEC) Flat Panel Display Devices Technical Committee, in Plasma Display Panels - Part 2-2: Measuring Methods − Optoelectrical, (IEC 61988 2-2 ed1.0) (IEC, Geneva, Switzerland, 2003).
17. S. H. Yoo, T. J. Kweon, H. K. Kwon, and E. G. Heo, "The improvement of ambient contrast in plasma display panel using subtractive mixture of colors," SID Symposium Digest **37**, 1217-1220 (2006).